

## Original Article

# A novel transverse talar tunnel achieved less vessel damage and better drilling safety for ATFL reconstruction: a cadaveric study with three-dimensional microCT

Dingyu Wang<sup>1,2</sup>, Zhongcheng Shen<sup>2</sup>, Shuai Yang<sup>1</sup>, Bo Zhang<sup>1</sup>, Yanzhang Li<sup>1</sup>, Yin Fang<sup>3</sup>, Chen Jiao<sup>1</sup>, Qinwei Guo<sup>1</sup>, Weiguang Zhang<sup>2</sup>, Dong Jiang<sup>1</sup>

<sup>1</sup>Institute of Sports Medicine, Beijing Key Laboratory of Sports Injuries, Peking University Third Hospital, Beijing 100191, P. R. China; <sup>2</sup>Department of Human Anatomy and Histology and Embryology, Peking University, Beijing 100191, P. R. China; <sup>3</sup>Division of Bioengineering, School of Chemical and Biomedical Engineering, Nanyang Technological University, Singapore 637457, Singapore

Received August 6, 2020; Accepted November 3, 2020; Epub December 15, 2020; Published December 30, 2020

**Abstract:** Purpose: To introduce a novel transverse tunnel (TT) in anterior talofibular ligament (ATFL) reconstruction, and assess whether it was superior to the tunnels currently used. Methods: Thirteen fresh cadaveric lower extremities were perfused with lead-based contrast. Talar tunnels were drilled from the ATFL insertion in the following directions: transversely towards the medial side (TT), towards the talar neck (TNT), and towards the anterior, distal, and posterior points of the medial malleolus (AMMT, DMMT, and PMMT, respectively). MicroCT was used to reconstruct the tali, and virtual transosseous and 20-mm blind-ended tunnels were generated. The graft bending angle, vascular compromise caused by the tunnels, and the minimum distances from the tunnels to the chondral surfaces were evaluated. Results: The bending angles between the ATFL and the TT, TNT, AMMT, DMMT, and PMMT were  $47.3\pm 7.9^\circ$ ,  $41.5\pm 7.7^\circ$ ,  $57.0\pm 6.0^\circ$ ,  $63.9\pm 11.7^\circ$ , and  $87.9\pm 6.2^\circ$ , respectively. The proportion of damaged intraosseous vessels was significantly less for the TT ( $7.8\pm 2.7\%$ ) compared with the AMMT ( $10.0\pm 5.2\%$ ), DMMT ( $15.5\pm 6.5\%$ ), and PMMT ( $16.9\pm 3.9\%$ ). Both the TNT and the AMMT carried a high risk of joint penetration, with respective minimum distances of  $2.2\pm 1.7$  mm and  $1.4\pm 1.0$  mm from the tunnel to the cartilage; in contrast, the TT, DMMT, and PMMT had larger safety margins, with minimum distances of  $5.4\pm 0.8$  mm,  $8.9\pm 2.7$  mm, and  $6.0\pm 1.2$  mm. The blind-ended tunnels caused less vascular compromise and had larger minimum distances to the cartilage (better drilling safety) than the transosseous tunnels for all tunnel directions. Conclusion: The TT achieves a superior graft bending angle and intraosseous blood supply protection than the AMMT, DMMT, and PMMT, and is less likely to result in cartilage damage than the TNT. The 20-mm blind-ended tunnels achieve less vessel damage and better drilling safety than transosseous tunnels.

**Keywords:** Ankle ligament reconstruction, bone tunnel, blood supply, safety, microCT

## Introduction

Ankle sprains are common injuries in athletes and in the general population [1]. The lateral ankle ligaments are most commonly involved, especially the anterior talofibular ligament (ATFL) and the calcaneofibular ligament [2]. Up to 40% of patients with a lateral ankle sprain develop chronic lateral ankle instability [3]. If conservative treatment fails to restore the stability of the ankle joint, surgical lateral ankle ligament repair or reconstruction is required.

The indications for ligament reconstruction include poor quality ligament remnants, long-term ankle instability, failed previous ATFL repair, high-demand ankle activity, and high-grade ligamentous laxity [4].

Among ATFL reconstruction strategies, anatomic reconstruction remains the gold standard [5, 6]. The consensus is that the entrance of the tunnel should be the anatomic attachment of the ATFL, but the tunnel direction varies among studies [7-10]. During talar tunnel cre-

## A novel transverse talar tunnel for ATFL reconstruction

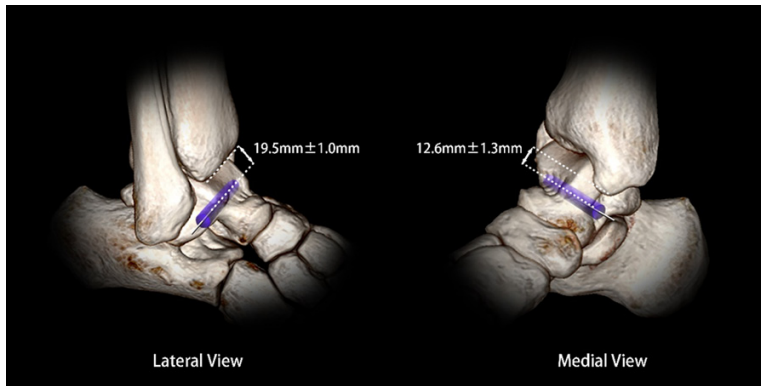


**Figure 1.** Illustration of the novel transverse tunnel. The transosseous tunnel is parallel to the plantar plane and distal anterior margin of the tibia, and crosses the talus in a transverse direction. The mean distance between the tunnel and the distal anterior margin of the tibia was  $19.5\pm 1.0$  mm, and the mean distance between the tunnel and the medial malleolus was  $12.6\pm 1.3$  mm.

ation, it is crucial to ensure that the drill does not penetrate the cartilage. The tunnel is commonly drilled towards the medial malleolus (MM), as this direction carries a relatively low risk of penetration into the joint [7-11]. A radiological study showed that it is safest to direct the tunnel towards the most posterior point of the MM [12]. However, in ATFL reconstruction with a tunnel directed towards the MM, the graft must make an acute bend at the entrance of the tunnel, forming a “killer turn”. The acute turn causes repetitive friction between the graft and bony tunnel, and might result in increased laxity, as seen in posterior cruciate ligament (PCL) reconstruction [13, 14]. In addition, because of the special nature of the talar blood supply, there is a risk of necrosis after talar surgery [15]. One study has reported multiple cystic formations along the drilling tunnel in the talus [16]. Studies of the intraosseous vessels of the talus show that a tunnel directed towards the MM passes through the nutrition vessels of the talar body, and might destroy more blood vessels than a tunnel directed towards the talar neck [17-19].

It remains unclear which talar tunnel direction is superior regarding the graft bending angle, vascular compromise effect, and drilling safety (i.e., the likelihood of the drill penetrating the chondral surface). Based on our previous MicroCT study, we rationally designed a talar tunnel for ATFL reconstruction. The objective of

this study is to introduce this novel transverse tunnel (TT) in ATFL reconstruction, and assess whether it was superior to the tunnels currently used.

### Materials and methods

This study was approved by our local ethics committee (IRB00006761-M2019164). Thirteen single fresh cadaveric lower extremities were investigated, including 10 males and 3 females. Six tali were from right limbs, and 7 were from left limbs. The average donor age was 61 years (range 50 to 79 years).

Specimens with lower extremity trauma, previous knee surgery, paralysis, vascular disease including atherosclerosis, diabetes mellitus, skeletal deformities, leukemia, and long periods of bedrest before death were excluded. Lead tetroxide (Sinopharm Chemical Reagent Beijing Co., Ltd.) was ground up, and the particles were sieved. Lead tetroxide particles less than  $40\ \mu\text{m}$  in diameter were suspended in turpentine oil (Chemical Reagent Beijing Co., Ltd.) at ratios of 1:1.5 (w/v), 1:1 (w/v), and 1:0.5 (w/v). The femoral arteries were cannulated and perfused with 90 mL of 1:1.5, 60 mL of 1:1, and 15 mL of 1:0.5 contrast. The skin of the toe was incised to confirm terminal perfusion.

Surgery was performed with the ankle joint in a neutral relaxed position. We first dissected and identified the center of the ATFL insertion and then used a straight K-wire to drill through the talus with a drilling guide (Micro Vector, Smith & Nephew). The TT was created from the talar insertion of the ATFL towards the medial side, parallel to the distal anterior margin of the tibia and the plantar plane (**Figure 1**). The mean distance between the TT and the distal anterior margin of the tibia was  $19.5\pm 1.0$  mm, and the mean distance between the TT and the MM was  $12.6\pm 1.3$  mm. Five different tunnels were drilled in each specimen. The other tunnels were drilled towards the following external landmarks: the deepest point of the talar neck in

## A novel transverse talar tunnel for ATFL reconstruction

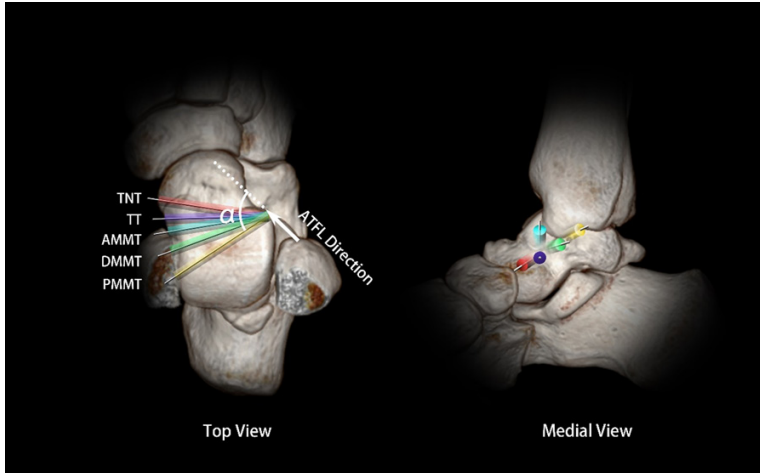


**Figure 2.** Illustration showing all five talar tunnels. The tunnels all start at the anterior talofibular ligament (ATFL) insertion site, and are then directed towards the talar neck (TNT; red), the medial side running parallel to the distal anterior margin of the tibia and the plantar plane (TT; purple), the most anterior point of the medial malleolus (AMMT; blue), the most distal point of the medial malleolus (DMMT; green), and the most posterior point of the medial malleolus (PMMT; yellow). The graft bending angle ( $\alpha$ ) is defined as the angle between the natural ATFL and the tunnel on the top view.

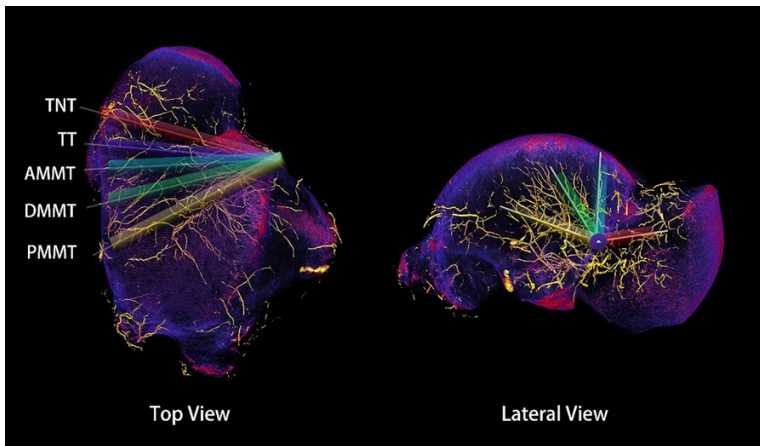


**Figure 3.** A high-resolution reconstructed talus model with intraosseous vessels used to examine the effect of each tunnel on the intraosseous blood supply. The transverse tunnel (TT; purple) runs parallel to most vessels, and the presence of abundant anastomosed vessels minimizes the damage to the blood supply. The tunnel directed toward the most distal point of the medial malleolus (DMMT; green) and the tunnel directed toward the most posterior point of the medial malleolus (PMMT; yellow) pass through the vessels and affect the blood supply to the talar body and talar dome.

the anteromedial corner (TNT), the most anterior point of the MM (AMMT), the most distal point of the MM (DMMT), and the most posterior point of the MM (PMMT) (Figure 2). The angle between the K-wire and the ATFL was measured as the graft bending angle ( $\alpha$  in Figure 2).

vessel - damaged proportion

$$= \frac{\text{vessel - damaged volume of the talus}}{\text{volume of the whole talus}} \times 100\%.$$

The minimum distances between each tunnel and the talar head cartilage, talar dome cartilage, and subtalar cartilage were measured to

The tali were harvested and scanned using a microCT scanner (Inveon, Siemens Ltd., USA). The acquisition protocols were: CT scan setup (total rotation, 360°; rotation steps, 360), X-ray detector setup (transaxial, 2,048; axial, 2,048; exposure time, 1,500 ms; binning: 1), system magnification (low), and X-ray tube setup (voltage, 80 kV; current, 500 mA). The down-sampling factor used in the reconstruction was 2. The effective voxel size was 52.30  $\mu\text{m}$ . The grayscale ranges for the vessel were determined by morphological observations. The vessel ranges were 3,400 to 32,760 HU. The smallest arteries that could be identified were approximately 40  $\mu\text{m}$ .

Virtual tunnels were generated in a 3D bone model in accordance with the K-wire tunnels (Figure 3). The diameter of the tunnels was 5 mm. Both a transosseous tunnel and a 20-mm blind-ended tunnel were generated. The vascular compromise effect was evaluated in each talus (red area in Figures 4, 5). The vessel-damaged portions in the 13 specimens were overlaid, so that the concentration of the red color represented the relative risk of vascular compromise. The volume of the whole talus and its vessel-damaged portion were measured. The proportion of the vessel-damaged volume was calculated as:

## A novel transverse talar tunnel for ATFL reconstruction

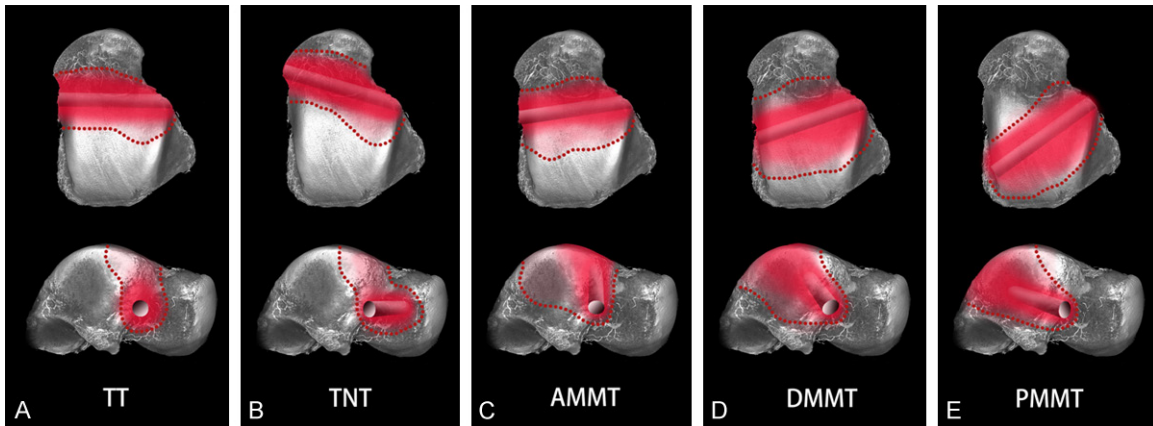


**Figure 4.** Vascular compromise caused by the transosseous tunnels (n = 13). A. Transverse tunnel (TT); B. Tunnel directed towards the talar neck (TNT); C. Tunnel directed towards the anterior point of the medial malleolus (AMMT); D. Tunnel directed towards the distal point of the medial malleolus (DMMT); E. Tunnel directed towards the posterior point of the medial malleolus (PMMT).

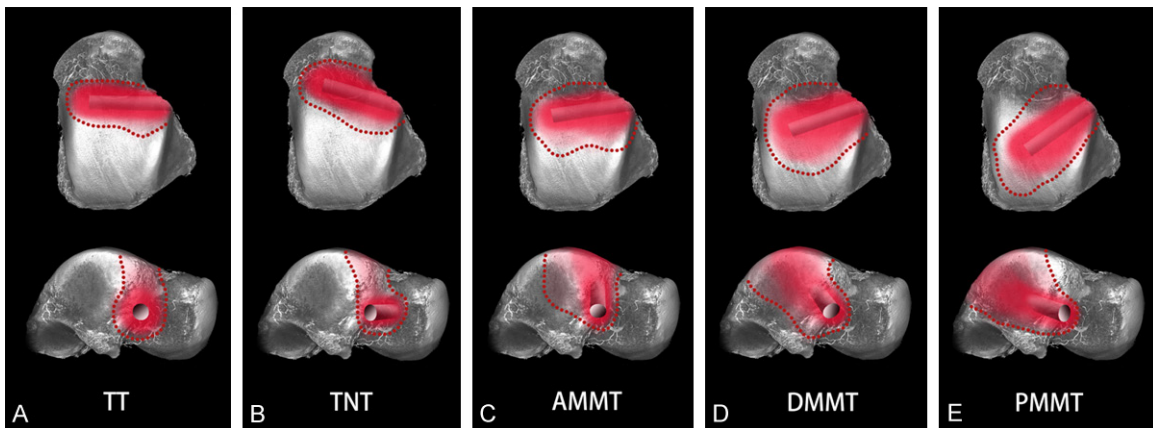


**Figure 5.** Vascular compromise caused by the 20-mm blind-ended tunnels (n = 13). A. Transverse tunnel (TT); B. Tunnel directed towards the talar neck (TNT); C. Tunnel directed towards the anterior point of the medial malleolus (AMMT); D. Tunnel directed towards the distal point of the medial malleolus (DMMT); E. Tunnel directed towards the posterior point of the medial malleolus (PMMT).

evaluate the safety of the drilling. The minimum distances from the TT and the TNT to the bony surface of the superior talar neck were also measured.

### Statistical analysis

The vessel volume was analyzed using SPSS 24.0 (IBM, USA). The paired t-test was used to compare the vessel-damaged proportions caused by each of the tunnels. One-way ANOVA was used to analyze the graft bending angles created by the five tunnels. Tukey's multiple comparisons test was used to analyze the differences between the tunnels. A two-tailed *p* value of < 0.05 was considered statistically significant.

## Results

### Graft bending angle at the tunnel entrance

**Table 1** shows the graft bending angle at the tunnel entrance for each of the five tunnel types ( $\alpha$  in **Figure 2**). The graft bending angle at the TT entrance ( $47.3 \pm 7.9^\circ$ ) was larger than that at the TNT entrance ( $41.5 \pm 7.7^\circ$ ) ( $P = 0.015$ ). The graft bending angles of the AMMT, DMMT, and PMMT were significantly higher than that of the TT ( $P < 0.05$ ).

### Vascular compromise caused by each of the tunnels

The 3D vascular model of the talus showed that the vascular compromise effect differed

# A novel transverse talar tunnel for ATFL reconstruction

**Table 1.** Summary of the results for each of the five tunnels

Tunnel direction	Graft bending angle	Vessel-compromising area	Safety	Comments
TT	47.3° ± 7.9°	minimal effect, near the tunnel	Safe	Ideal tunnel
TNT	41.5° ± 7.7°	minimal effect, near the tunnel	Transosseous tunnel easily penetrates talar head cartilage	Unsafe and impractical (hard to palpate the landmark on skin)
AMMT	57.0° ± 6.0°	talar neck and anterior 1/3 of talar dome cartilage	K-wire probably penetrates medial talar dome shoulder cartilage	High risk of penetrating into the ankle joint
DMMT	63.9° ± 11.7°	majority of the talar body and talar dome cartilage	Safe	Greatly damage the blood supply
PMMT	87.9° ± 6.2°	majority of the talar body and talar dome cartilage	Potential risk of posteromedial neurovascular bundle injury	Potential “killer turn” effect, unsafe and greatly damage the blood supply

TT: transverse tunnel running parallel to the distal anterior margin of the tibia and the plantar plane; TNT: tunnel directed toward the deepest point of the talar neck; AMMT: tunnel directed toward the anterior point of the medial malleolus; DMMT: tunnel directed toward the distal point of the medial malleolus; PMMT: tunnel directed toward the posterior point of the medial malleolus.

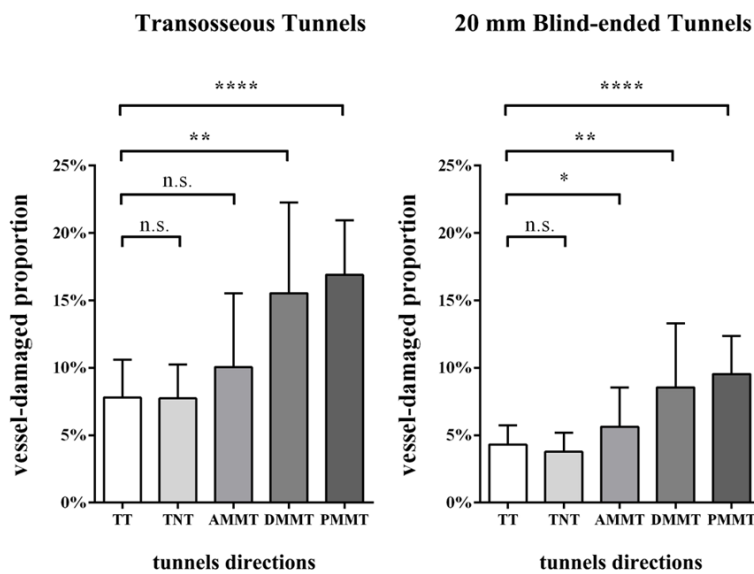


**Figure 6.** Proportion of the talus with damaged intraosseous vessels caused by the transosseous and blind-ended tunnels in all five tunnel directions (n = 13). TT: transverse tunnel running parallel to the distal anterior margin of the tibia and the plantar plane; TNT: tunnel directed toward the deepest point of the talar neck; AMMT: tunnel directed toward the anterior point of the medial malleolus; DMMT: tunnel directed toward the distal point of the medial malleolus; PMMT: tunnel directed toward the posterior point of the medial malleolus.

between the transosseous and blind-ended tunnels (Figures 4, 5). The TT had a minimal effect on the vessels because it ran parallel to most vessels, and the abundant anastomosed vessels provided supplementary blood supply. Additionally, the TT barely affected the blood supply of the talar dome cartilage. However, the AMMT affected the blood supply of the talar neck and the anterior 1/3 of the talar dome cartilage. Both the DMMT and the PMMT passed through the vessels and damaged the vessels supplying the majority of the talar body

and half of the cartilage. Compared with the transosseous tunnels, the 20-mm blind-ended tunnels caused significantly less vascular compromise and preserved the blood supply of the medial talar body and cartilage.

Quantitative analysis also demonstrated that the transosseous tunnels damaged significantly more vessels than the 20-mm blind-ended tunnels for all five of the tunnel types (P < 0.001; Figure 6). The TT damaged 7.8±2.7% of the talar blood supply, which was similar to the damage caused by the TNT (7.7±2.4%, P = 0.901) and the AMMT (10.0±5.2%, P = 0.054), but significantly less than that caused by the DMMT (15.5±6.5%, P = 0.000) and the PMMT (16.9±3.9%, P = 0.000).

The 20-mm blind-ended TNT also caused the least vascular compromise, damaging 4.3±1.4% of the blood supply, which was significantly less than the damage caused by the AMMT (5.6±2.8%, P = 0.040), DMMT (8.5±4.6%, P = 0.001), and PMMT (9.5±2.7%, P = 0.000).

### Drilling safety

The minimum distances from each of the tunnels to the three articular surfaces of the talus are shown in Table 2. The minimum distances

## A novel transverse talar tunnel for ATFL reconstruction

**Table 2.** Drilling safety of the tunnels assessed by the minimum distance (mm)

N = 13	Directions	Tunnel depth	Minimal distance (mm)		
			Talar head cartilage	Talar dome cartilage	Subtalar cartilage
Transosseous tunnels	TT	32.2±1.1	5.4±0.8	10.5±1.7	7.2±1.5
	TNT	34.1±2.0	2.3±1.7*	10.8±1.9	7.4±1.5
	AMMT	32.5±2.4	13.2±1.9	1.4±1.0*	13.1±1.6
	DMMT	33.1±2.4	15.2±1.5	8.9±2.7	9.7±1.9
	PMMT	36.5±4.3	14.8±1.2	9.0±2.4	6.0±1.2
Blind-ended tunnels	TT	20	14.4±1.5	10.5±1.7	7.3±1.3
	TNT	20	14.4±2.4	10.8±1.9	7.5±1.4
	AMMT	20	13.3±1.9	6.8±1.0	13.1±1.6
	DMMT	20	15.1±1.7	10.7±1.5	10.1±2.3
	PMMT	20	14.8±1.2	13.1±1.0	6.3±1.3

Values are shown as mean ± SD. \*High risk of penetration into the joint.

from the TT and TNT to the bony surface of the superior talar neck was namely 6.8±1.6 mm and 7.5±1.5, considered adequate to prevent penetration. The TT, DMMT, and PMMT had adequate minimum distances to all three articular surfaces, suggesting good safety. The transosseous TNT was close to the talar head cartilage, with a minimum distance of 2.3±1.7 mm. The transosseous AMMT was at risk of penetrating the talar dome cartilage, with a minimum distance of 1.4±1.0 mm to the talar dome. Overall, the 20-mm blind-ended tunnels had greater minimum distances between the tunnel and the bony surface of the superior talar neck and the three articular surfaces than the transosseous tunnels for all five tunnel directions.

### Discussion

The present study assessed the novel transverse talar tunnel using microCT, and showed that it may be a viable option in ATFL reconstruction due to its smaller graft bending angle, less vascular compromise, and low probability of joint penetration in comparison with currently used tunnel directions. Compared with the transosseous tunnels, all of the 20-mm blind-ended tunnels caused less intraosseous vessel damage and were less likely to penetrate into the joint. The transosseous TT has been used in our institute, with good clinical outcomes. In contrast to the tunnels drilled towards the MM, the drilling direction of the TT was just parallel to the anterior edge of the tibia and the plantar plane; this was feasible and repeatable, and no intraoperative guide was needed. The present

study confirmed the potential of the TT as a preferable alternative in ATFL reconstruction.

The bending angle of the reconstructed ATFL was 47.3±7.9° for the TT, which was significantly smaller than the bending angles for the AMMT, DMMT, and PMMT. In particular, the graft bending angle of the PMMT was nearly 90°, forming a “killer turn” similar to the acute bend of the PCL graft around the proximal posterior tibia resulting from the transtibial tunnel technique in PCL reconstruction. In PCL reconstruction, a more acute bending angle of the graft entering the tunnel increases the risk of abrasion against the anterior ‘lip’ of the internal tibial tunnel aperture [20]. We consider that such a sharp turn of the ATFL graft in the talus would also increase the stresses on the interface between the graft and the tunnel, causing graft elongation and tunnel entrance enlargement. Our results suggest that the PMMT may increase the graft bending angle, while the TT and the TNT decrease the effect of the “killer turn”; however, this requires confirmation in further biomechanical and clinical studies.

The TT caused less vascular compromise compared with the other tunnel directions. The talus receives its major blood supply from the vessel ring around the talus neck, with the ring mainly located in the tarsal sinus and tarsal canal [17, 21]. The vessels then travel a long distance from the tarsal sinus and tarsal canal to the talar body and cartilage dome. Although the TT damaged the vessels in the talar neck, the presence of the anastomosed vessel ring around the neck meant that the blood supply

## A novel transverse talar tunnel for ATFL reconstruction

was only affected in the area near the tunnel; the vessels supplying the talar body and cartilage dome were not damaged. In contrast, the AMMT, DMMT, and PMMT damaged the vessels with fewer anastomoses, which may affect the blood supply of the talar body and subchondral area. The quantitative analysis also revealed that the TT compromised fewer intraosseous vessels than the other tunnels. The blind-ended TT showed a similar superiority over the other tunnels, and caused even less vascular compromise than the transosseous TT. Thus, overall, the 20-mm blind-ended TT caused the least intraosseous vessel damage and best preserved the blood supply of the talar dome cartilage compared with the other tunnel types.

The safety of drilling in the talus must also be considered; this comprises outer safety by avoiding the neurovascular bundle and tendons around the talus, and inner safety by leaving sufficient distance to avoid penetrating the cartilage. In the Asian cadavers used in the present study, the transosseous TNT and AMMT resulted in the highest risk of cartilage perforation. In addition, the transosseous PMMT might damage the posteromedial neurovascular bundle. However, the TT had sufficient distance from the joint surface, which resulted in a relatively low risk of joint penetration; this has also been shown on postoperative CT of patients who underwent ATFL reconstruction using the TT in our institute. In the present study, the tunnel length was nearly the same as that in the Caucasian patients in a previous study [12]. This previous study compared the inner safety of five drilling directions (towards the talar neck, and towards the anterior, distal, medial, and posterior points of the MM) with three depths (20 mm, 25 mm, and 30 mm) [12]. The authors reported that all of the 30-mm-deep tunnels were located beyond the minimum safe distance from the bone surface, while all of the 20-mm-deep tunnels except the tunnel directed towards the anterior point of the MM were safe [12]. Our findings suggest that the 20-mm blind-ended TT should be recommended based on its low risk of joint penetration. However, the clinical operability of this blind-ended TT needs further study.

Many studies have reported satisfactory clinical outcomes for ATFL reconstruction [4, 6, 22, 23]. but it is unclear whether different tunnel directions affect the clinical outcomes. Cromb e et al. drilled the talar tunnel towards the middle

of the talus, and found that tiny differences between the talar tunnel angles and directions affect the clinical outcomes [7]. The authors reported that the lateral talar tunnel ratio (defined as the ratio between the distance from the talar tunnel entrance to the talonavicular joint and the maximal length of the talus on the lateral view) was significantly lower in patients with a good clinical outcome than in those with a poor clinical outcome [7]. Further studies comparing the clinical outcomes of different tunnel directions are needed.

The present study simultaneously evaluates and compares the graft bending angle, vascular compromise effect, and drilling safety of various tunnel directions in ATFL reconstruction in Asian cadavers with relatively small tali. The 20-mm blind-ended TT achieved the best outcomes, and may be recommended as a new drilling strategy. The strengths of the present study are the novel high-resolution microCT quantitative analysis of the vascular compromise effect, and the thorough examination of all aspects, including the graft bending angle, blood supply, and drilling safety.

### Limitation

The present study also had limitations. First, the average donor age was 61 years (range 50-79 years), which is older than the typical population requiring ATFL reconstruction. Second, a cadaveric study cannot accurately reflect the reaction of the human body and vessels to the drilling damage. Third, due to the small diameter of the K-wire, we did not examine its vascular compromise effect. It should also be noted that plantarflexion or dorsiflexion could change the tunnels' positions in the bone, although drilling should be performed towards the externally palpable surgical landmarks. Thus, the safety of drilling and the vascular compromise effect may change if the plantarflexion or dorsiflexion is changed. Finally, although the present study reported the graft bending angle and vascular compromise effect of tunnels drilled in different directions, the effect on the postoperative outcomes needs to be studied.

### Conclusion

The TT achieves a superior graft bending angle and intraosseous blood supply protection than the AMMT, DMMT, and PMMT, and is less likely

to cause cartilage damage than the TNT. The 20-mm blind-ended tunnels achieve less vessel damage and better drilling safety than transosseous tunnels.

### Acknowledgements

The study was funded by the National Key Research and Development Program of China (2018 YFF0301100); Recipient: NA. The Natural Science Foundation of Beijing, China (19L2133); Weiguang Zhang is the grand recipient. Peking University Medicine Seed Fund for Interdisciplinary Research and the Fundamental Research Funds for the Central Universities (BMU2020MX020); Chen Jiao is the grand recipient.

### Disclosure of conflict of interest

None.

**Address correspondence to:** Dong Jiang, Institute of Sports Medicine, Beijing Key Laboratory of Sports Injuries, Peking University Third Hospital, Beijing 100191, P. R. China. Tel: +86-13811280948; E-mail: bysyjiangdong@126.com; Weiguang Zhang, Department of Human Anatomy and Histology and Embryology, Peking University, Beijing 100191, P. R. China. Tel: +86-13683145110; E-mail: zhangwg@bjmu.edu.cn

### References

- [1] Gribble PA, Bleakley CM, Caulfield BM, Docherty CL, Fourchet F, Fong DT, Hertel J, Hiller CE, Kaminski TW, McKeon PO, Refshauge KM, Verhagen EA, Vicenzino BT, Wikstrom EA and Delahunt E. Evidence review for the 2016 International Ankle Consortium consensus statement on the prevalence, impact and long-term consequences of lateral ankle sprains. *Br J Sports Med* 2016; 50: 1496-1505.
- [2] Vuurberg G, Hoorntje A, Wink LM, van der Doelen BFW, van den Bekerom MP, Dekker R, van Dijk CN, Krips R, Loogman MCM, Ridderikhof ML, Smithuis FF, Stufkens SAS, Verhagen EALM, de Bie RA and Kerkhoffs GMMJ. Diagnosis, treatment and prevention of ankle sprains: update of an evidence-based clinical guideline. *Br J Sports Med* 2018; 52: 956.
- [3] O'Loughlin PF, Murawski CD, Egan C and Kennedy JG. Ankle instability in sports. *Phys Sportsmed* 2009; 37: 93-103.
- [4] Dierckman BD and Ferkel RD. Anatomic reconstruction with a semitendinosus allograft for chronic lateral ankle instability. *Am J Sports Med* 2015; 43: 1941-1950.
- [5] Yasui Y, Shimozone Y and Kennedy JG. Surgical procedures for chronic lateral ankle instability. *J Am Acad Orthop Surg* 2018; 26: 223-230.
- [6] Noailles T, Lopes R, Padiolleau G, Gouin F and Brillhault J. Non-anatomical or direct anatomical repair of chronic lateral instability of the ankle: a systematic review of the literature after at least 10 years of follow-up. *Foot Ankle Surg* 2018; 24: 80-85.
- [7] Crombé A, Borghol S, Guillo S, Pesquer L and Dallaudiere B. Arthroscopic reconstruction of the lateral ankle ligaments: radiological evaluation and short-term clinical outcome. *Diagn Interv Imaging* 2019; 100: 117-125.
- [8] Wang W and Xu GH. Allograft tendon reconstruction of the anterior talofibular ligament and calcaneofibular Ligament in the treatment of chronic ankle instability. *BMC Musculoskeletal Disord* 2017; 18: 150.
- [9] Michels F, Cordier G, Burssens A, Vereecke E and Guillo S. Endoscopic reconstruction of CFL and the ATFL with a gracilis graft: a cadaveric study. *Knee Surg Sports Traumatol Arthrosc* 2016; 24: 1007-1014.
- [10] Clanton TO, Campbell KJ, Wilson KJ, Michalski MP, Goldsmith MT, Wijdicks CA and LaPrade RF. Qualitative and quantitative anatomic investigation of the lateral ankle ligaments for surgical reconstruction procedures. *J Bone Joint Surg Am* 2014; 96: e98.
- [11] Higashiyama R, Aikawa J, Iwase D, Takamori Y, Watanabe E and Takaso M. Anatomical arthroscopic anterior talofibular ligament and calcaneofibular ligament reconstruction using an autogenic hamstring tendon: safe creation of anatomical fibular tunnel. *Arthrosc Tech* 2019; 8: e215-e222.
- [12] Michels F, Guillo S, Vanrietvelde F, Brugman E and Stockmans F. How to drill the talar tunnel in ATFL reconstruction? *Knee Surg Sports Traumatol Arthrosc* 2016; 24: 991-997.
- [13] Weimann A, Wolfert A, Zantop T, Eggert AK, Raschke M and Petersen W. Reducing the "killer turn" in posterior cruciate ligament reconstruction by fixation level and smoothing the tibial aperture. *Arthroscopy* 2007; 23: 1104-1111.
- [14] Kim SJ, Shin JW, Lee CH, Shin HJ, Kim SH, Jeong JH and Lee JW. Biomechanical comparisons of three different tibial tunnel directions in posterior cruciate ligament reconstruction. *Arthroscopy* 2005; 21: 286-293.
- [15] Babu N and Schuberth JM. Partial avascular necrosis after talar neck fracture. *Foot Ankle Int* 2010; 31: 777-780.
- [16] Jeong SY, Kim JK and Lee KB. Is retrograde drilling really useful for osteochondral lesion of talus with subchondral cyst?: a case report. *Medicine (Baltimore)* 2016; 95: e5418.
- [17] Wang D, Shen Z, Fang X, Jiao C, Guo Q, Hu Y, Yu J, Jiang D and Zhang W. Vascular compromise

## A novel transverse talar tunnel for ATFL reconstruction

- ing effect of drilling for osteochondral lesions of the talus: a three-dimensional micro-computed tomography study. *Arthroscopy* 2019; 35: 2930-2937.
- [18] Oppermann J, Franzen J, Spies C, Faymonville C, Knifka J, Stein G and Bredow J. The microvascular anatomy of the talus: a plastination study on the influence of total ankle replacement. *Surg Radiol Anat* 2014; 36: 487-494.
- [19] Miller AN, Prasarn ML, Dyke JP, Helfet DL and Lorich DG. Quantitative assessment of the vascularity of the talus with gadolinium-enhanced magnetic resonance imaging. *J Bone Joint Surg Am* 2011; 93: 1116-1121.
- [20] Li Y, Zhang J, Song G, Li X and Feng H. The mechanism of "killer turn" causing residual laxity after transtibial posterior cruciate ligament reconstruction. *Asia Pac J Sports Med Arthrosc Rehabil Technol* 2016; 3: 13-18.
- [21] Prasarn ML, Miller AN, Dyke JP, Helfet DL and Lorich DG. Arterial anatomy of the talus: a cadaver and gadolinium-enhanced MRI study. *Foot Ankle Int* 2010; 31: 987-993.
- [22] Li H, Hua Y, Li H and Chen S. Anatomical reconstruction produced similarly favorable outcomes as repair procedures for the treatment of chronic lateral ankle instability at long-term follow-up. *Knee Surg Sports Traumatol Arthrosc* 2020; 28: 3324-3329.
- [23] Lee KT, Park YU, Kim JS, Kim JB, Kim KC and Kang SK. Long-term results after modified Brostrom procedure without calcaneofibular ligament reconstruction. *Foot Ankle Int* 2011; 32: 153-157.